Robust approach to study the effect on quantum phase transitions of various perturbations at finite temperatures

Cheng-Pu Lv,[1] Yan-Chao Li,[1,2,*] and Hai-Qing Lin[2,3]

[1]*Center of Materials Science and Optoelectronics Engineering, College of Materials Science and Opto-Electronic Technology, University of Chinese Academy of Sciences, Beijing 100049, China*

[2]*Beijing Computational Science Research Center, Beijing 100193, China*

[3]*Department of Physics, Beijing Normal University, Beijing 100875, China*

(Received 13 January 2022; revised 8 February 2022; accepted 8 February 2022; published 22 February 2022)

We propose using maximum coherence (QC_{max}) to study quantum phase transition (QPT). We investigate several well-known models, such as the XXZ model, J_1-J_2 model, and one-dimensional spin Kitaev model. The results show that QC_{max} can be used to detect different types of QPTs, including the Berezinskii-Kosterlitz-Thouless and topological types. In addition, QC_{max} is more robust against interferences, such as thermal fluctuations and measurement interferences, than any existing detector. This property enables QC_{max} to identify QPTs in experiments, where temperature effects and measurement interferences always exist. Thus, QC_{max} might be an ideal tool for studying QPTs because of its measurability, universality, and robustness against interferences.

DOI: 10.1103/PhysRevB.105.054424

I. INTRODUCTION

Quantum phase transition (QPT) [1] plays a very important role in condensed matter physics. Understanding this process is beneficial in exploring the microscopic mechanism behind various macroscopic phenomena of materials. The discovery of magnetically mediated superconductivity in a heavy-fermion system [2] and the superfluid–Mott insulator phase transition for an ultracold-atom system [3] greatly enhanced our interest in QPT studies.

Given the inherited quantum nature, a close link is generally believed to exist between QPT and quantum information. This link has been widely explored and elucidated. A good example is the success in describing QPT of the XY model by the concurrence [4]. Studying QPT based on the quantum information is advantageous and has led to the fast development in this field, because no prior knowledge on the order parameter of the system is needed for this process. By contrast, prior knowledge is required for the traditional Ginzburg-Landau symmetry breaking theory [1]. Many concepts adopted from quantum information have been used as detectors to characterize QPTs. These concepts include the von Neumann entropy (E_v) [5], fidelity and its related fidelity susceptibility [6,7], quantum discord (QD) [8,9], and quantum coherence (QC) [10,11]. Two main issues exist for this process. One is to find a universal physical quantity as a detector that can identify all kinds of QPTs, and the other one is to experimentally achieve this process. Resolving these issues will not only improve the extensive development and deep understanding of QPT study but will also help in determining the mechanism of a QPT, the essence of genuine quantumness, and the relationship between quantumness and QPT. The results might be useful in determining how to control quantumness using a QPT in a quantum computer.

However, such a detector has not yet been successfully determined. Comprehensive studies have shown that any previous proposed detector has limitations on uniquely characterizing different kinds of QPTs, such as in detecting the Berezinskii-Kosterlitz-Thouless (BKT)-type QPT in the XXZ model and the critical point (CP) at $J_2 \approx 0.241$ of the J_1-J_2 model [12,13]. Moreover, most related works have only performed theoretical studies, and few factors, such as thermal fluctuation and measurement interference, have been considered for experimentation. Although QD and QC have been applied to detect QPTs at finite temperature (T) [9,14–16], these quantities were only tested under some specific conditions. Their universality needs further study.

In this paper, we propose using maximum quantum coherence (QC_{max}) as a QPT detector. We investigated its performance on three main aspects of QPT study, namely, its effectiveness on detecting different types QPTs, robustness against thermal fluctuations during experiments, and ability against a measurement interference. Compared with other detectors, QC_{max} is advantageous in all aspects. Thus, it may serve as an ideal tool to theoretically and experimentally study QPTs.

II. INTERACTION ANISOTROPY CAUSED QPTS

A. The XXZ Model

The Hamiltonian for the XXZ model is defined as follows:

$$H_{\mathrm{XXZ}} = \sum_{j}^{N} \sigma_j^x \sigma_{j+1}^x + \sigma_j^y \sigma_{j+1}^y + \Delta \sigma_j^z \sigma_{j+1}^z, \tag{1}$$

where N is the number of spins in the chain, Δ describes the anisotropy of the spin-spin interaction, and σ_j are the usual Pauli matrices at site j. This model has two critical points at $T = 0$, namely, a continuous BKT-type phase transition at $\Delta = 1$, and a first-order transition caused by the ground state level crossing at $\Delta = -1$ [17].

*ycli@ucas.ac.cn

 ©2022 American Physical Society

We use the transfer matrix renormalization group (TMRG) technique to simulate an infinite XXZ spin chain. This method is based on a Trotter-Suzuki decomposition of the partition function of a system and can directly handle infinite chains [18]. The reduced density matrix ρ_{ab} for the nearest neighbors a and b can be obtained from a set of thermal averages of correlation functions [19,20]. Then, all QPT detectors $\mathcal{C}$, E_v, QD, and QC can be obtained from ρ_{ab} as follows:

(1) The concurrence between a and b, $\mathcal{C}(\rho_{ab}) = \max\{0, \lambda_1 - \lambda_2 - \lambda_3 - \lambda_4\}$, where λ_n ($n = 1, 2, 3$, and 4) are the square roots of the eigenvalues of $\rho_{ab}\tilde{\rho}_{ab}$ in descending order, and $\tilde{\rho}_{ab} = (\sigma_a^y \otimes \sigma_b^y)\rho_{ab}^*(\sigma_a^y \otimes \sigma_b^y)$ is the time-reversed matrix of ρ_{ab} [4].

(2) The entanglement entropy E_v, $E_v(\rho_{ab}) = -\mathtt{Tr}\rho_{ab}\mathtt{ln}\rho_{ab}$ [5].

(3) The QD, $\mathcal{D}(\rho_{ab}) = E_v(\rho_b) + \min_{\{b_k\}} \widetilde{E}_v(\rho_{ab}|\{b_k\}) - E_v(\rho_{ab})$, where $\widetilde{E}_v(\rho_{ab}|\{b_k\}) = \sum_k p_k E_v(\rho_{ab}^k)$ with $\rho_{ab}^k = \frac{1}{p_k}\ (I \otimes b_k)\rho_{ab}(I \otimes b_k)$ and $p_k = \mathtt{Tr}[(I \otimes b_k)\rho_{ab}(I \otimes b_k)]$ is the conditional entropy, and the minimum is achieved from a complete set of projective measures $\{b_k\}$ on site b [9,21,22].

(4) The last detector QC is related to a specific observable K, such as σ_x. The K coherence of a quantum state is defined as follows:

$$I(\rho_{ab}, K) = -\tfrac{1}{4}Tr[\rho_{ab}, K]^2, \tag{2}$$

where [...] denotes the commutator. For state ρ_{ab}, if we choose the observable at a, K is then written as $K_a \bigotimes I_b$ [23].

The measurable quantity QC reflects the information of a state skewed to the observable. Given the possible anisotropy and different bond interactions in a system, the value of QC must depend on measurement directions and positions. For a quantum system, there must be competitions from different quantum states and the final exhibition must be the dominant one. Therefore, to well reflect the coherence condition and its relationship with QPTs, we should consider the maximum QC in the system. That is, instead of a given measurement direction and position [10], we should measure the QC on different directions and positions to capture the dominant coherence condition. There are three cases: (i) For an anisotropic system, we consider the spin operator σ_n with an arbitrary direction $\vec{n}$ to reconstruct the quantum coherence, the maximum of which reflects the maximum skewed information and will be used as a new detector for the QPT study. We name this quantity $\mathrm{QC_{max}}$, which is determined as follows:

$$\mathrm{QC_{max}} = \max \mathrm{I}(\rho_{\mathrm{ab}}, \sigma_{\mathrm{n}}) = \max -\tfrac{1}{4}\mathrm{Tr}[\rho_{\mathrm{ab}}, \sigma_{\mathrm{n}}]^2. \tag{3}$$

Given that the observable σ_n is

$$\sigma_n = \begin{pmatrix} \cos\theta & \sin\theta e^{-i\varphi} \\ \sin\theta e^{i\varphi} & -\cos\theta \end{pmatrix}, \tag{4}$$

the maximum is determined by traversing θ from 0 to π and φ from 0 to 2π. (ii) For an isotropic system but with different bond interactions, the value of QC is independent of measurement directions. The difference of coherence is just from measured positions. Thus, the $\mathrm{QC_{max}}$ is gotten by comparing different coherences on different interacted bonds. (iii) For a system with both anisotropy and different bond interactions, both case (i) and case (ii) should be considered. The $\mathrm{QC_{max}}$ is gotten by comparing σ_n QCs in different directions and different interacting bonds.

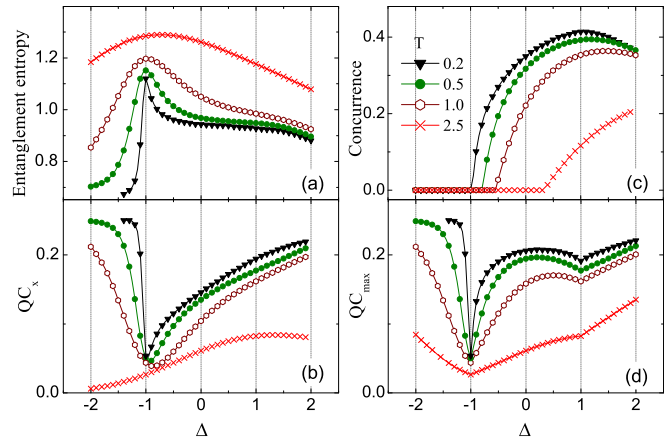

FIG. 1. (a) Entanglement entropy E_v, (b) σ^x coherence $\mathrm{QC_x}$, (c) concurrence $\mathcal{C}$, and (d) the maximum quantum coherence $\mathrm{QC_{max}}$ [see Eq. (3)] at different temperatures ($T = 0.2$, 0.5, 1.0, and 2.5) are plotted as functions of Δ. Plotted data in all figures are dimensionless.

For comparison, we plot $\mathrm{QC_{max}}$ and other detectors for the XXZ model under different T in Fig. 1. At very low temperatures, the first-order critical point at $\Delta = -1$ is clearly identified by the singularity of E_v and σ^x coherence $\mathrm{QC_x}$, as shown in Figs. 1(a) and 1(b), respectively. However, the singular behavior quickly becomes a round peak and disappears as temperature increases. For the continuous-order phase transition at $\Delta = 1$, E_v and $\mathrm{QC_x}$ do not exhibit any signatures even at very low temperatures. For the concurrence $\mathcal{C}$, although this quantity shows apparent signatures of QPT at low temperatures, it is zero at $\Delta = -1$ and reaches maximum at $\Delta = 1$; both signatures lose their ability to identify QPTs as temperature increases [Fig. 1(c)]. This behavior is consistent with the results from Refs. [9,10].

By contrast, $\mathrm{QC_{max}}$ shows an excellent behavior in identifying QPTs [Fig. 1(d)]. The two critical points are clearly signatured by the singular behaviors even at very high temperatures. This remarkable feature of $\mathrm{QC_{max}}$ shows absolute superiority over the other detectors. Here, $\mathrm{QC_{max}}$ yields an efficiency equivalent to that of the QD in Refs. [9,10]. QD measures the minimum difference of two expressions of mutual information. Thus, QD actually reflects the influence of measured directions to the quantum correlation. Similarly, the proposed $\mathrm{QC_{max}}$ also reflects the influence but based on quantum coherence. However, the singularity of QD does not always correspond to a QPT as shown in Ref. [24]. This singularity actually peaks at a noncritical point in the Su-Schrieffer-Heeger (SSH) model with interactions [25], while the singularity of $\mathrm{QC_{max}}$ always corresponds to the transition points (the results are not shown here). Therefore, $\mathrm{QC_{max}}$ might be more credible than QD as a QPT detector. In addition, although the quantum coherence spectrum was proposed to detect the QPTs of the XXZ model [26], as a direct extension of the definition of quantum coherence based on Wigner-Yanase-Dyson skew information, $\mathrm{QC_{max}}$ possesses the original meaning of quantum coherence to measure the

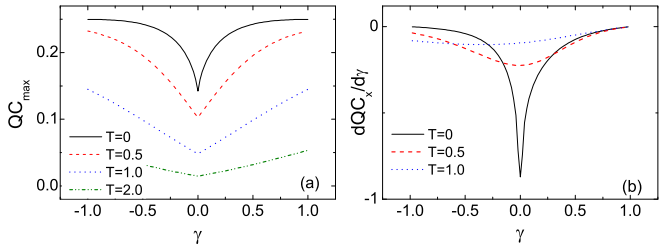

FIG. 2. (a) The maximum quantum coherence QC_{max} as a function of γ at $N = 2001$, $\lambda = 0.5$, and different values of T; (b) derivative of σ_x quantum coherence QC_x with respect to γ at $\lambda = 0.5$ and different values of T.

key resource in quantum information theory. Compared with the quantum coherence spectrum, there is a more general understanding and application for QC_{max} in plenty of fields, such as quantum optics, quantum calculation, and information processing. QC_{max} can also be implementable experimentally with current technology [15]. Therefore, we believe it is a better detector choice for QPTs.

B. The XY Model

We studied the XY model to further demonstrate the effectiveness of QC_{max} in detecting QPTs. Its Hamiltonian is as follows:

$$H_{XY} = \sum_{j=1}^{N}\left(\frac{1+\gamma}{2}\sigma_j^x\sigma_{j+1}^x + \frac{1-\gamma}{2}\sigma_j^y\sigma_{j+1}^y + \lambda\sigma_j^z\right), \quad (5)$$

where N, σ^x, σ^y, and σ^z are the same as those in Eq. (1), γ describes the anisotropy in the spin-spin interaction on the XY plane, and λ is the external magnetic field. This model can be exactly diagonalized [1], and the two-site reduced density matrix ρ_{ab} needed for the calculations of the QPT detectors were obtained in Ref. [27].

This model possesses two distinct critical regions, namely, the critical line along $\gamma = 0$ between $-1 < \lambda < 1$ and the continuous critical lines lines along $|\lambda| = 1$ [28,29]. Similar to the XXZ model, the CP along $\gamma = 0$ is also caused by anisotropy. Therefore, CP might be detected directly by QC_{max}. Given that the anisotropy only comes from the XY plane, we focus n in Eq. (4) on this plane, i.e., we set $\theta = \pi/2$ and take φ changing from 0 to 2π. The results are shown in Fig. 2. Two particular features are notable. First, the valleys of QC_{max} clearly indicate the critical points at $\gamma = 0$, as shown in Fig. 2(a) for $\lambda = 0.5$. This behavior remedies the defect of QC, including the σ_x coherence QC_x and σ_y coherence QC_y. Contrary to other detectors, such as entanglement and fidelity, QC_x and QC_y need the peak of their derivatives other than themselves to spotlight the CPs [10,16]. In addition, the CP can be precisely identified by QC_{max} regardless of the size of the system, while the pseudocritical phenomenon cannot be avoided for QC when N is small [29]. Second, QC_{max} detects the critical point at different T values [Fig. 2(a)], while the peak of $dQC_x/d\gamma$ disappears as temperature increases, namely, it cannot detect the CP anymore [Fig. 2(b)].

III. LATTICE STRUCTURE ASYMMETRY CAUSED QPTS

The QPTs discussed above are caused by interaction anisotropy. Similarly, if the cause of a QPT is from the asymmetry of the lattice structure, then QC_{max} should be achieved by comparing QCs along two competing driving bonds.

The first example is the one-dimensional SSH model [30]. Its Hamiltonian is written as follows:

$$H_S = -\sum_j (1+\eta)c_{B,j}^\dagger c_{A,j} + (1-\eta)c_{A,j+1}^\dagger c_{B,j} + \text{H.c.}, \quad (6)$$

where A and B are sublattice indices, and η denotes the dimerization. A topological phase exists at $\eta < 0$, while a topological trivial phase exists at $\eta > 0$.

Following the solution of the XXZ model, we use the TMRG numerical method to determine the reduced density matrix for the two sublattices A and B by replacing the spin-up and spin-down states with the occupied and empty ones, respectively. Then, we choose the observable in Eq. (2) as $c^\dagger + c$, namely, the transformation of a state between occupied and empty, and QC_{max} can be obtained directly. The results are shown in Fig. 3(a). No derivative or size-dependent scaling analysis, similar to that performed for the QC [16], is necessary. The topological critical point is directly indicated by the singularity of QC_{max} even at high T.

The second example is the one-dimensional spin Kitaev model [31], with its Hamiltonian determined as follows:

$$H = \sum_j^N \left(J_1\sigma_{2j-1}^x\sigma_{2j}^x + J_2\sigma_{2j}^y\sigma_{2j+1}^y\right), \quad (7)$$

where J_1 and J_2 describe the spin-spin interactions alternatively along the chain (J_1 is set to 1 as the energy unit). This model has a topological QPT at $J_2 = 1$, and this QPT is separated by two states containing two hidden string orders. We calculate QC_{max} (the maximum of QC from spins connected by J_1 and J_2) using the TMRG method. The results of QC_{max} under different temperatures are plotted in Fig. 3(b). The singularity of the QC_{max} curve clearly identifies the topological CP even at a relative high T.

The third example is the spin-1/2 antiferromagnetic Heisenberg J_1-J_2 model, and its Hamiltonian is as follows:

$$H = \sum_{j=1}^N (J_1\mathbf{S}_j\cdot\mathbf{S}_{j+1} + J_2\mathbf{S}_j\cdot\mathbf{S}_{j+2}), \quad (8)$$

where $\mathbf{S}_j$ denotes a spin-1/2 operator at site j. This model has a BKT-type QPT at $J_2^c \approx 0.241$, which is controlled by a marginal operator and difficult to observe [13,32,33]. At a special point, the Majumdar-Ghosh (MG) point, $J_2/J_1 = 0.5$, the model has an exact analytical solution. Its ground state is the uniformly weighted superposition of two nearest-neighbor dimer states [34]. We use the TMRG method to process an infinite chain. QC_{max} (the maximum of σ^x QCs from J_1 and J_2 connected spins) is shown in Figs. 3(c) and 3(d). The MG point is clearly spotlighted by the singularity even at relatively high temperatures. Meanwhile, a round peak appears at the left side of the MG point at relatively low T, namely, $T = 0.2$ [Figs. 3(c)]. As T further decreases, the peak is promoted and moves toward $J_2 \approx 0.24$ [Fig. 3(d)], which clearly indicates the BKT-type CP of this model.

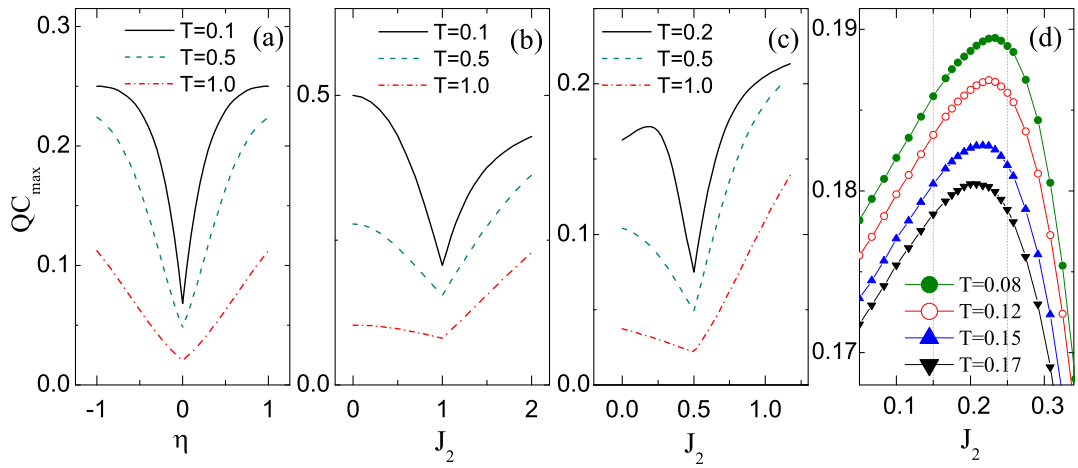

FIG. 3. QC_{max} as functions of driving parameters at different values of T: (a) SSH model, (b) one-dimensional spin Kitaev model, and (c) and (d) spin J_1-J_2 model [(d) shows the behavior of the round peak near $J_2 = 0.2$ in (c) at lower temperatures].

IV. DETECTING QPTS AGAINST INTERFERENCE

Any measurements related to QPTs should consider not only the influence of temperature but also the interference, such as the coupling of a probe to the system. A possible way to detect QPTs or control qubits on quantum computations and quantum communications is the interacting of a probe or ancillary control qubit with the system [35]. Thus, the influence of the ancilla on the quantum states of the system cannot be neglected. Therefore, assuming that the interference comes from the probe, we study the influence of the environment on different detectors in detecting QPTs.

First, we consider the XY and XXZ models, where the anisotropy leads to the QPTs. The Hamiltonians of these models can be unified as follows:

$$H = H_o + H', \tag{9}$$

where H_o represents the original Hamiltonian of the XY and XXZ models in Eqs. (1) and (5), respectively, and H' is the probing term. To unchange the driving source of QPTs, $H' = \delta\sigma_I^z\sigma_A^z$ for the XY model and $H' = \delta\sigma_I\sigma_A$ for the XXZ model, and σ_I and σ_A are the Pauli matrices of the probe I and an arbitrary measured site A of the system, respectively. The superscript z indicates that only the z direction is chosen, while δ describes the interaction strength between I and A. The two-site reduced density matrix refers to site A and its nearest neighbor.

The results from the exact diagonalization (ED) for $N = 16$ are shown in Fig. 4. The CP at $\gamma = 0$ for the XY model is always indicated by the turning point of QC_{max} [Fig. 4(a)], while for the other detector, the minimum of $dQC_x/d\gamma$ goes away from the CP as δ increases [Fig. 4(b)]. The same result is observed for the XXZ model. The BKT-type QPT at $\Delta = 1$ is precisely indicated even at relatively high δ values [Fig. 4(c)], while the round peak of the concurrence, which is a possible indicator for the QPT [Fig. 1(c)], moves to the right side of the critical point as δ is increased [Fig. 4(d)].

Second, we consider the spin SSH model, where the lattice structure asymmetry causes the QPTs. The Hamiltonian of this model is as follows:

$$H = -\sum_j (1+\eta)\left(\sigma_{2j-1}^x\sigma_{2j}^x + \sigma_{2j-1}^y\sigma_{2j}^y\right) + (1-\eta)\left(\sigma_{2j}^x\sigma_{2j+1}^x + \sigma_{2j}^y\sigma_{2j+1}^y\right) + \delta\sigma_I^z\sigma_A^z, \tag{10}$$

where η denotes the dimerization similar to that in the spinless SSH model, and δ, σ_I^z, and σ_A^z have the same definitions as those in Eq. (9). Similar to that in the spinless SSH model, this system has a topological QPT at $\eta = 0$ when the interference term is absent.

The exact diagonalization results are plotted in Figs. 4(e) and 4(f). For the SSH model studied here, QC_{max} is defined as the bigger one of the two neighboring QCs. The valley in Fig. 4(e) remains at $\eta = 0$ as δ increases. This phenomenon clearly illustrates the effectiveness of QC_{max} in detecting QPT against the interference. For comparison, the results of

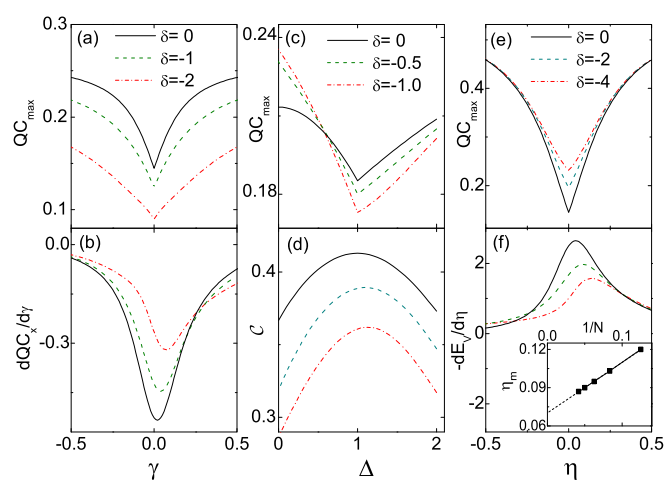

FIG. 4. QC_{max} as functions of driving terms under different strengths of measurement interference δ and $N = 16$ for (a) XY, (c) XXZ, and (e) spin SSH models. The second row shows the results of the other detectors for the same models and values of δ: (b) $dQC_x/d\gamma$, (d) concurrence $\mathcal{C}$, and (f) $-dE_v/d\eta$. The inset in (f) shows the scaling behavior of the peak position η_m of $-dE_v/d\eta$.

$-dE_v/d\eta$ at the same values of δ are plotted in Figs. 4(f), in which the peak of $-dE_v/d\eta$ moves away from the CP as δ increases. The results of $dQD/d\eta$ show a behavior similar to that of $-dE_v/d\eta$ (not shown here). These quantities cease to reflect the occurrence of the QPT.

In addition, to overcome the finite-size effect, $-dE_v/d\eta$ at $\delta = -4$ under different N values are calculated. The CP deviation of the peak always exists as N increases. The peak position η_m (here, the η value of the pseudo CP, that is the peak position of $-dE_v/d\eta$ at $\delta = 0$, is subtracted from the value of η_m to avoid the influence of the pseudo CP.) does not vanish even at the thermodynamic limit [as $N \to \infty$, the extrapolated value is 0.07 as shown in the inset of Fig. 4(f)]. This phenomenon indicates that the deviation of the peak of $-dE_v/d\eta$ from the CP is due to δ, not to the finite-size effect. The same behavior exists in QD. Thus, QC_{max} is more robust against interference than other detectors to have practical significance in the study of QPT.

V. SUMMARY

In summary, several types of QPTs in different systems are studied using TMRG, ED, and analytical methods. QC_{max}, instead of QC, can precisely identify the QPTs caused by anisotropy or asymmetrical lattice structures. The BKT-type QPT in the J_1-J_2 model was also indicated. Moreover, the QC_{max} can not only detect QPTs at finite T as effective as QD but can also indicate QPTs under a measurement interference, while other detectors, including QD, lose their ability. We explain the mechanism as follows: QC_{max} catches the maximum information that skewed to the observable, making it more comprehensive than QC itself in reflecting the changes of a quantum state. Moreover, QC_{max} considers not only the anisotropy similar to the QD but also the lattice asymmetry. This characteristic leads to the more robust behavior of QC_{max} against measurement interference than QD. Given that temperature perturbations and measurement interferences cannot be avoided in an experiment, QC_{max} may serve as a potential ideal detector for QPTs.

ACKNOWLEDGMENTS

We acknowledge financial support from the National Natural Science Foundation of China (Grant No. 12074376 and No. 52072365), the Beijing Municipal Natural Science Foundation (Grant No. 1222027), the NSAF (Grant No. U1930402), the Fundamental Research Funds for the Central Universities, and the International Partnership Program (Grant No. 211211KYSB20180020) of the Chinese Academy of Sciences.

[1] S. Sachdev, *Quantum Phase Transition* (Cambridge University Press, Cambridge, 1999).
[2] N. D. Mathur, F. M. Grosche, S. R. Julian, I. R. Walker, D. M. Freye, R. K. W. Haselwimmer, and G. G. Lonzarich, Nature (London) **394**, 39 (1998).
[3] M. Greiner, O. Mandel, T. Esslinger, T. W. Hänsch, and I. Bloch, Nature (London) **415**, 39 (2002).
[4] A. Osterloh, Luigi Amico, G. Falci, and Rosario Fazio, Nature (London) **416**, 608 (2002).
[5] S. J. Gu, S. S. Deng, Y. Q. Li, and H. Q. Lin, Phys. Rev. Lett. **93**, 086402 (2004).
[6] P. Zanardi and N. Paunkovic, Phys. Rev. E **74**, 031123 (2006).
[7] W. L. You, Y. W. Li, and S. J. Gu, Phys. Rev. E **76**, 022101 (2007).
[8] M. S. Sarandy, Phys. Rev. A **80**, 022108 (2009).
[9] T. Werlang, C. Trippe, G. A. P. Ribeiro, and G. Rigolin, Phys. Rev. Lett. **105**, 095702 (2010).
[10] G. Karpat, B. Çakmak, and F. F. Fanchini, Phys. Rev. B **90**, 104431 (2014).
[11] I. Marvian and R. W. Spekkens, Phys. Rev. A **90**, 062110 (2014).
[12] S. Chen, L. Wang, Y. Hao, and Y. Wang, Phys. Rev. A **77**, 032111 (2008).
[13] S. Chen, L. Wang, S. J. Gu, and Y. Wang, Phys. Rev. E **76**, 061108 (2007).
[14] T. Baumgratz, M. Cramer, and M. B. Plenio, Phys. Rev. Lett. **113**, 140401 (2014).
[15] D. Girolami, Phys. Rev. Lett. **113**, 170401 (2014).
[16] Y. C. Li and H. Q. Lin, Sci. Rep. **6**, 26365 (2016).
[17] M. Takahashi, *Thermodynamics of One-dimensional Solvable Models* (Cambridge University Press, Cambridge, 1999).
[18] I. Peschel, X. Wang, M. Kaulke, and K. Hallberg, *Density-Matrix Renormalization: A New Numerical Method in Physics* (Springer, New York, 1999), pp. 149–172; U. Schollwock, Rev. Mod. Phys. **77**, 259 (2005).
[19] Y. C. Li and S. S. Li, Phys. Rev. B **78**, 184412 (2008).
[20] O. F. Syljuåsen, Phys. Rev. A **68**, 060301(R) (2003).
[21] H. Ollivier and W. H. Zurek, Phys. Rev. Lett. **88**, 017901 (2001).
[22] R. Dillenschneider, Phys. Rev. B **78**, 224413 (2008).
[23] E. P. Wigner and M. M. Yanase, Proc. Natl. Acad. Sci. USA **49**, 910 (1963).
[24] Z. Y. Sun, L. Li, K. L. Yao, G. H. Du, J. W. Liu, B. Luo, N. Li, and H. N. Li, Phys. Rev. A **82**, 032310 (2010).
[25] W. C. Yu, Y. C. Li, P. D. Sacramento, and H. Q. Lin, Phys. Rev. B **94**, 245123 (2016).
[26] Y. C. Li, J. Zhang, and H. Q. Lin, Phys. Rev. B **101**, 115142 (2020).
[27] Y. C. Li and H. Q. Lin, Phys. Rev. A **83**, 052323 (2011).
[28] E. H. Lieb, T. D. Schultz, and D. C. Mattis, Ann. Phys. **16**, 407 (1961); S. Katsura, Phys. Rev. **127**, 1508 (1962); P. Pfeuty, Ann. Phys. **57**, 79 (1970).
[29] S. L. Zhu, Phys. Rev. Lett. **96**, 077206 (2006).
[30] R. Wakatsuki, M. Ezawa, Y. Tanaka, and N. Nagaosa, Phys. Rev. B **90**, 014505 (2014).
[31] X. Y. Feng, G. M. Zhang, and T. Xiang, Phys. Rev. Lett. **98**, 087204 (2007).
[32] M. Thesberg and E. S. Sørensen, Phys. Rev. B **84**, 224435 (2011).
[33] S. J. Gu, H. Li, Y. Q. Li, and H. Q. Lin, Phys. Rev. A **70**, 052302 (2004).
[34] C. K. Majumdar and D. K. Ghosh, J. Math. Phys. **10**, 1388 (1969); **10**, 1399 (1969).
[35] G. M. D'Ariano and P. Perinotti, Phys. Rev. Lett. **94**, 090401 (2005).